Received: 04 March 2023, Accepted: 31 March 2023

Original Research

Journal of Advanced Veterinary Research
(2023) Volume 13, Issue 2, 277-287

Detection of Avian Leukosis Virus Subgroup J in Egyptian Ducks and Chicken Using Molecular and Histopathological Approach and Allocation of Genetic Mutations and Recombination Events in the *Env*elope Protein Gene *gp85*

Yousef A. Soliman[1], Maha A.N. Gamal[1], Eman M.S. El-Nagar[2], Marwa S. Khattab[3], Heba M. Salem[4*]

[1]Central Laboratory for Evaluation of Veterinary Biologics (CLEVB), Agriculture Research Center (ARC). Cairo, Egypt.

[2]Veterinary Serum and Vaccine Research Institute (VSVRI), Agriculture Research Center (ARC). Cairo, Egypt.

[3]Department of Pathology, Faculty of Veterinary Medicine, Cairo University; Giza, 12211, Egypt.

[4]Department of Poultry Diseases, Faculty of Veterinary Medicine, Cairo University, Giza 12211, Egypt.

***Correspondence**
Heba M. Salem
E-mail address: dr.hebasalem@cu.edu.eg

Abstract

Avian leukosis virus (ALV) is an oncogenic contagious virus infecting different avian species. This study aims to molecularly detect the circulating strains of ALV in various chicken and duck farms at different Egyptian governorates. Freshly dead birds were exposed for postmortem examination (PM) then samples were processed for histopathological examination as well as molecular detection of ALV using qRT-PCR and sequence analysis of the *env*elope glycoprotein gene (*gp85*) surface protein antigen with detection of recombination events that might be found between the detected strains. PM revealed the existence of diffuse enlargement of most internal organs, and in some cases, nodular enlargement was observed. Histopathological investigation showed myeloid cells infiltration of eosinophilic granular cytoplasm in the examined tissues. Five molecularly positive samples were sequenced and submitted in the GenBank with accession numbers MZ614719, MZ614720, MZ614721, MZ614722, and MZ614723. The phylogenetic tree construction based on the sequenced *gp85* gene revealed that all Egyptian isolates were nearly arranged in a single branch despite the year of collection and were phylogenetically distant from other sequences. In general, studies concerning the genetic diversity of *gp85*, and the recombination events concluded that the ALV-J virus is a wide host range involving both chicken and ducks. Because ALV causes serious financial problems to threaten poultry production and neither vaccines nor treatment tools are now available for ALV prevention and control, periodical molecular monitoring with whole genome sequence and analysis for the circulating strains with ethical eradication of the positive birds are recommended to overcome such a problem.

KEYWORDS
ALV, *Env*elope protein, *gp85*, qRT-PCR, Histopathology.

INTRODUCTION

Avian leukosis virus (ALV) is a financially important, vertically transmitted oncogenic retrovirus affecting egg-laying and broiler chickens, ducks, and even wild birds; it may contaminate poultry vaccines (Wu *et al*., 2022).

ALV is taxonomically classified as genus alpharetrovirus within the Retroviridae family, Subfamily Orthoretrovirinae (Tang *et al*., 2022). Based on the *env*elope glycoprotein antigen interference, host range, and cross-neutralization pattern, exogenous ALV was classified into subgroups: A-E and J (Bande *et al*., 2016). On the other hand, the ALV subgroups E-H and I were classified as endogenous viruses (McNally *et al*., 2010). It has been thought that ALV subgroup J transmitted vertically more frequently in broiler breeders than other classical ALV subgroups (Qu, *et al*., 2016).

ALV is described as an *env*eloped, spherical to pleomorphic, 80-100 nm in diameter virus with monopartite, linear, dimeric, positive sense ssRNA genome of about 7200 bp, with a 5′-cap and a 3′poly-A tail; there were long terminal repeats (LTR) have been detected in the viral genome with a size of 600 nt at both 5′ and 3′ ends, the LTRs contain the U3, U5, and R regions, a polypurine tract (PPT) is found at the 3′end and a primer-binding site (PBS) at the 5′end (Qiao *et al*., 2021).

ALV-J is thought to have emerged through a recombination event that might occur between an unknown exogenous subgroup of the ALV parent virus and an endogenous retrovirus (Sacco, *et al*., 2004), and the virus prototype strain (HPRS-103) was first isolated from broiler chickens in the UK (Li, *et al*., 2020).

ALV invades the host cell through the *env*elope glycoprotein gp95, which is cleaved into two chains, the surface glycoprotein (SU or *gp85*) and a transmembrane protein (TM or gp37) (Pan *et al*., 2012). This interaction triggered the refolding of gp37 and the activation of its fusogenic potential by unmasking its fusion peptide (Cheng *et al*., 2019). The fusion process begins at the host cell plasma membrane, the transmembrane protein (TM), which is classified as a class I viral fusion protein (Delos *et al*., 2005). The protein has nearly three conformational states based on the fusion stage, where the first stage is the pre-fusion native state, the second conformational state is the pre-hairpin intermediate state, and the last post-fusion hairpin state (Aydin *et al*., 2013). During the fusion process, the structure of the coiled-coil regions becomes trimer-of-hairpins, positioning the fusion peptide near the ectodomain at the C-terminal region (Aydin *et al*., 2013). This structure drive apposition and subsequent fusion of viral and tar-

ISSN: 2090-6277/2090-6269/

get cell membranes leading to the delivery of the viral nucleocapsid into the host cytoplasm (Aydin *et al*., 2013). The *env*elope glycoprotein gp95 is synthesized as an *Env*-Ryk chimeric protein, and then cellular protease cleaves this precursor into *gp85* and the putative oncogene gp69 (gp37-Ryk) (Jiang *et al*., 2014).

Host-specificity of each viral subgroup is determined by the *gp85* protein that forms globular structures on the viral surface and is involved in the process of viral binding (Meng *et al*., 2016, 2022) and has the most variable structure among other proteins of the ALV virus and exhibits high genetic diversity in the genome of ALV-J (Pan *et al*., 2012). The full-length *gp85* gene is estimated to have a 906-939 bp coding range for 302-313 amino acids polypeptide (33 KDa) (Deng *et al*., 2021). Previous studies revealed the presence of regions of sequence variability (hr1, hr2, vr1, vr2, and vr3) (Zeng *et al*., 2014a); the principal receptor interaction determinants were the hr1 and hr2 domains. At the same time, the vr3 plays an important role in the specificity determining of the receptor (Wang *et al*., 2018).

The Avian leukosis virus induces a variety of clinical signs among different avian species as ruffled feathers, emaciation, recumbence, and paleness in both comb and wattle with a drop in egg production in layer flocks (Kilany *et al*., 2015; Eid *et al*., 2019) also, the infections may result in a disturbance in cellular growth with subsequent neoplastic changes and primarily associated with myeloid leukosis (ML) (Qiao *et al*., 2021). Histopathological changes induced by ALV might vary greatly; it includes but are not limited to homogeneous lymphoblastosis (nodular or diffuse) in the liver and diffuse hepatic lymphocytic infiltration with mitotic figures (Wen *et al*., 2018). Neoplastic lymphocytes may accumulate, compress, and obliterate hepatic parenchyma, with round cells appearance, scanty cytoplasm, deep staining nuclei, distorted hepatic cords, and severely congested portal blood vessels (Li *et al*., 2009; Guo *et al*., 2010).

Given the nature of the virus in the induction of neoplastic changes and its host range expansion, it is indispensable to research the molecular evolution and detection of the recombination events between different strains isolated from different avian hosts (Shen *et al*., 2014). Therefore, the current study aimed to test the association of ALV-J in the tumor samples collected from chickens and ducks suffering from tumors, histopathological analysis of the associated tumors, and molecular analysis of the *gp85* surface protein antigen with the detection of recombination events that might be present among the isolated strains.

MATERIALS AND METHODS

Ethical approval

This work was approved by The Institutional Animal Care and Use Committee (IACUC) with the ethical number Vet CU 8/03/2022/409.

Samples

As mentioned in Table 1, samples were collected from 5 duck farms and 22 chicken farms from different Egyptian governorates including Gharbia, Damietta, Sharkia, and Dakahlia from Dec 2020 until March 2021. The investigated flocks have a history of variable mortalities with a drop in egg production in layer flocks with suspected tumor-like lesions in the internal organs especially liver, kidney, spleen, intestine, and ovary. From each examined farm, five freshly dead chickens were subjected to postmortem examination then tissue samples were collected from each bird including liver, kidney, pancreas, intestine, and ovary, after that a pool of each organ livers, spleens, kidneys, intestines, and ovaries were separately carried out, then processed either in 10 % neutral buffered formalin for histopathology or transported on ice directly to the lab and stored at -20°C for molecular analysis.

Histopathological analysis

Tissue specimens from the liver, kidney, pancreas, intestine, and ovary were collected and immediately fixed in 10 % formal saline, processed by paraffin embedding technique, sectioned (4 µm thick sections) by rotary microtome (Leica 2135, Germany), stained by hematoxylin and eosin (Bancroft and Gamble, 2008). A light microscope (Olympus Bx43, with DP 27 digital camera, Tokyo, Japan) was used to capture and examine microphotographs.

Molecular detection of the ALV by qRT-PCR

The existence of the ALV virus in the samples was tested by qRT-PCR amplification of the surface *env*elope gene (*gp85*). RNA extraction from tissue samples that showed tumor-like abnormalities in the PM examination was done using Trizol reagent (Thermo Scientific cat # 15596-026). RNA preparations were subjected to DNase treatment by incubation with 5 IU/µl DNase I (Biomatik Cat#A4193) at 25°C/30 min and then at 65°C/10 min.

Amplification was done using probe-based qRT-PCR Master Mix (Agilent Cat# 600809). Briefly, five ng of the purified RNA was mixed with the 12.5µl of RT-PCR master mix, 50 pmol of each forward and reverse primer, and 100 pmol of the probe in a 25µl final volume; ROX was used in each reaction as a passive reference dye for data normalization. The reaction condition was adjusted at 50°C/30 min and then at 95°C/15 min (one cycle each), and then at 95°C/20sec denature, 60°C/40 sec for both annealing, and extension (40 cycles). The fluorescent data were adjusted to be collected at the end of each extension cycle in the Ariamx thermal cycler (Agilent, Germany).

Sequencing analysis of the envelope protein gene (gp85) of ALV

The *gp85* gene 1st strand cDNA was synthesized from the purified, DNase-treated RNA samples using M-MuLV First Strand

Table 1. The tested bread and species collected from different governorates and their mean Cq values of qRT-PCR.

Governorate	Birds		No. of tested farms	Positive qRT-PCR		Mean Cq values of qRT-PCR from Organs			
	Species	Breed		No	%	Liver	Spleen	Intestine	ovary
Gharbia	Duck	breeders	5	1	20%	26.7	29.22	39.7	37.19
	chicken	breeders	5	1	20%	24.3	25.45	38.32	38.12
Damietta	chicken	indigenous layers	7	3	42.80%	21.02	23.56	39.16	29.25
Sharkia	chicken	breeders	6	1	16.60%	29.21	25.6	34.12	39.2
Dakahlia	chicken	breeders	4	1	25%	21.23	24.5	33.25	37.23

cDNA Synthesis (Biomatik cat# K5147); briefly, 50ng of the purified RNA was mixed with 10 nM of positive sense primer (Table 2) and 500µM/1µL of dNTP Mix (10 mM each) in a final volume of 14.5µl and incubated at 65°C/5min then on ice /1min, then 4µl of 5x RT buffer, 0.5µl of RNase Inhibitor (40 U/µl) and 1µl of M-MuLV Reverse Transcriptase (200 U/µl) was added. The 1st strand of cDNA was synthesized at 50°C/60min, and then the RT enzyme was inactivated at 85°C/5min.

PCR amplification of the *gp85* gene was then done using 5µl of cDNA, five µL of 10X high fidelity buffer (High Fidelity Hot Start Core Kit Jena Bioscience Cat # PCR 235S), 1µl of the dNTPs mix (2.5mM each) and 10 nM of each of primer that amplifies the *gp85* genes of ALV (Table 1). Finally, 0.5 µl of high-fidelity hot start pfu polymerase was added, and the PCR tubes were spun to collect down the fluid. The reaction was adjusted at 95°C/3 min for initial denature and 35 cycles of denaturing at 95°C/20 sec, annealing at 60°C/30 sec, and extension at 68°C/3 min using T professional 3000 thermal cyclers (Biometra, Germany).

Sequencing

Five strains were isolated from Dec 2020 to March 2021(Table 3) subjected to sequencing analysis of the *gp85* gene. The purity of the amplicons was checked on a 1% low melting agarose, and the size of the amplicons was determined using SynGene V4.01 (Synoptics – Cambridge- England). The correct bands were sliced off and purified (gel purification kit Biobasic - Canada cat #.BSC02S1).

The nucleotide sequence of the genes of the isolated ALV strains was performed in (LGC Germany) using ABI PRISM 3730XL Analyzer BigDyeTM Terminator Cycle Sequencing Kits using AmpliTaq DNA polymerase (FS enzyme Applied Biosystems). Single-pass sequencing was performed on each template using the amplification primer. Ethanol precipitation protocol was used to purify the fluorescent-labeled fragments from the unincorporated terminators. Samples were resuspended and electrophoresed in an ABI 3730xl sequencer (Applied Biosystems).

Analysis

The nucleotide sequences were analyzed and aligned using the MegAlign module of the Dynastar V15 software (Dnastar Inc., Madison, WI, USA) and aligned using the Clustal W module. The phylogenetic tree was constructed using Maximum likelihood (ML).

Analysis of the recombination events

Recombination events within each ALV-J strain isolated in the current study were analyzed according to the method of Martin (2009) (RDP-5 Program), the used algorisms including BootScan, MaxChi, GENECONV, SiScan, Chimaera, LARD, RDP, Phyl-Pro, and 3Seq, were employed for comparison (Martin *et al*., 2005a; b). Recombination events supported by four or more independent methods were only regarded as true positive events.

RESULTS

Clinical and postmortem findings

The investigated birds showed general signs of depression, ruffled feathers, emaciation, recumbence, and paleness in both comb and wattle, with a drop in egg production in layer flocks ranging from (15-35 %) in layer flocks, and reduced fertility and hatchability in the breeder flocks with mortalities ranged from (15- 25%).

Table 2. The primer sequences used in the current study.

Primer ID	Seq 5'→3'	Reference
	Primers used for amplification of *gp85* gene for sequencing	
ALV-J1	5'-GGATGAGGTGACTAAGAAAG-3'	Ottiger *et al*. (2010)
ALV-J2	5'-CGAACCAAAGGTAACACACG-3'	
	Primers used in qRT-PCR assay	
ALV-JNF	5'-TTGCAGGCATTTCTGACTGG-3'	Qin *et al*. (2013)
ALV-JNR	5'-ACACGTTTCCTGGTTGTTGC-3'	
ALV-JNP	5'-FAM-CCTGGGAAGGTGAGCAAGAAGGA- BHQ1 -3'	

Table 3. Isolates, designated names, and sequence Genbank accession numbers for the isolates used in the current study.

Strain name	Species	Type of production	Governorate	Isolate Designated name	Accession number
Avian leukosis virus *env* gene chicken Indigenous layers Damietta strain Egy/YA- 2021.3	Chicken	Layers	Damietta	Egy/YA- 2021.3	MZ614719
Avian leukosis virus *env* gene chicken breeders Sharqia strain Egy/YA- 2021.4	Chicken	Breeders	Sharqia	Egy/YA- 2021.4	MZ614723
Avian leukosis virus *env* gene duck Gharbia strain Egy/YA- 2021.9	Duck	Breeder	Gharbia	Egy/YA- 2021.9	MZ614720
Avian leukosis virus *env* gene chicken indigenous breeders Dakahlia strain Egy/YA- 2021.10	Chicken	Breeders	Dakahlia	Egy/YA- 2021.10	MZ614721
Avian leukosis virus *env* gene chicken Gharbia strain Egy/YA- 2021.14	Chicken	Breeders	Gharbia	Egy/YA-2021.14	MZ614722

The PM examination of the freshly dead chickens in the investigated flocks revealed the existence of diffuse nodular enlargement of chicken kidney, persistent bursa of Fabricius in breeder chicken (Fig. 1), and diffuse enlargement with subscapular hemorrhage in the liver of layer chicken with rupture in a pre-hepatic capsule of breeder chicken liver in some cases (Fig. 1). The spleen of the examined breeder chicken showed pale diffuse enlargement, and a ruptured spleen was observed in some examined chickens (Fig. 1). As seen in Figure 1, the pancreas revealed diffuse enlargement, and the ovaries of some examined layer chickens showed diffuse whitish color enlargement in the ovarian follicles. In contrast, the heart of some breeder chickens appeared severely enlargement chicken, and the intestine revealed severe thickening in the intestinal wall.

In the examined ducks, severe enlargement in the liver was observed with subscapular hemorrhage. In some cases, diffuse enlargement of the greenish-colored liver was noticed (Fig. 2), while the examined spleen showed severe enlargement with congestion, subscapular hemorrhage, and rupture in the splenic capsule. In some investigated ducks, diffuse enlargement in the liver

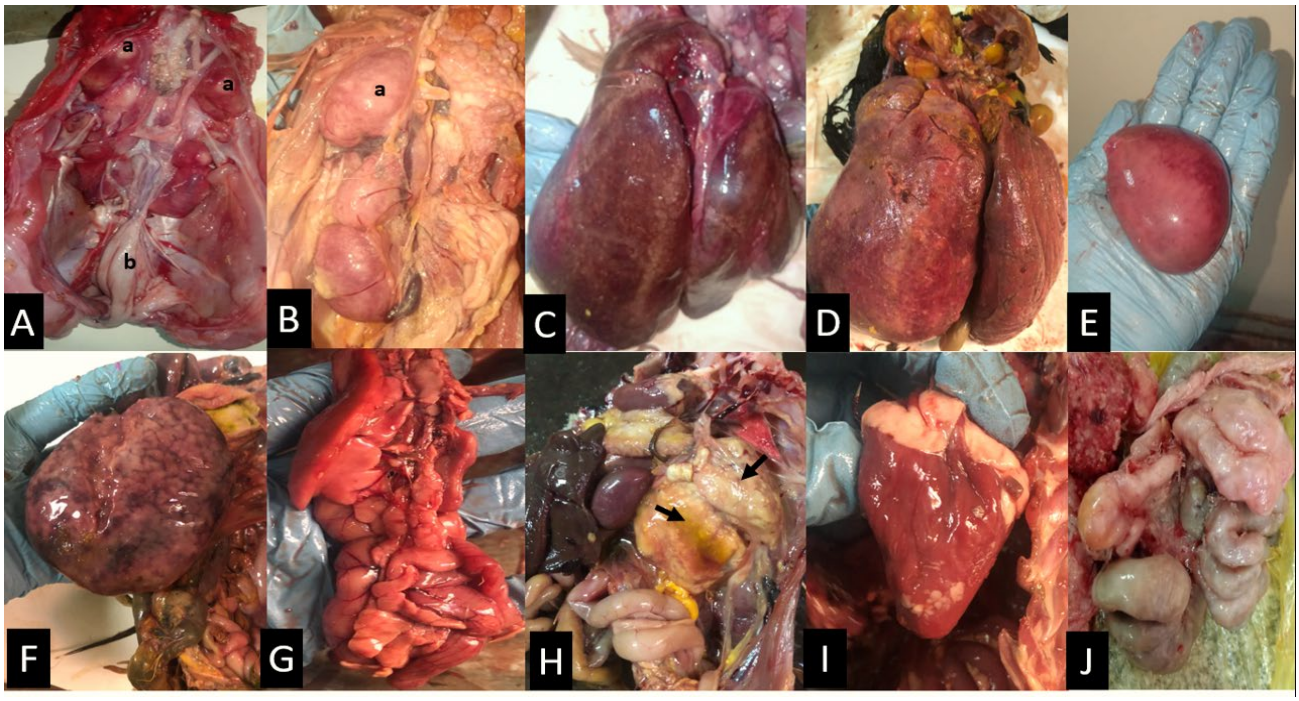

Fig. 1. Postmortem of freshly dead chickens shows: A: a, Diffuse nodular enlargement of layer chicken kidney; b: persistent bursa of Fabricius in breeder chicken; B: a, Diffuse enlargement with severe paleness in the kidney; C: Diffuse enlargement with subcapsular hemorrhage in the liver of layer chicken; D: Diffuse enlarged pale liver of breeder chicken with fatty degeneration; E: Diffuse enlargement in spleen of breeder chicken; F: Diffuse enlarged spleen with ruptured splenic capsule of layer chicken; G: Diffuse enlargement in layer chicken pancreas; H: Diffuse whitish color enlargement in the ovarian follicles of layer chicken (arrow); I: Severe enlargement in breeder chicken's heart; J: Severe thickening in the intestine of layer chicken.

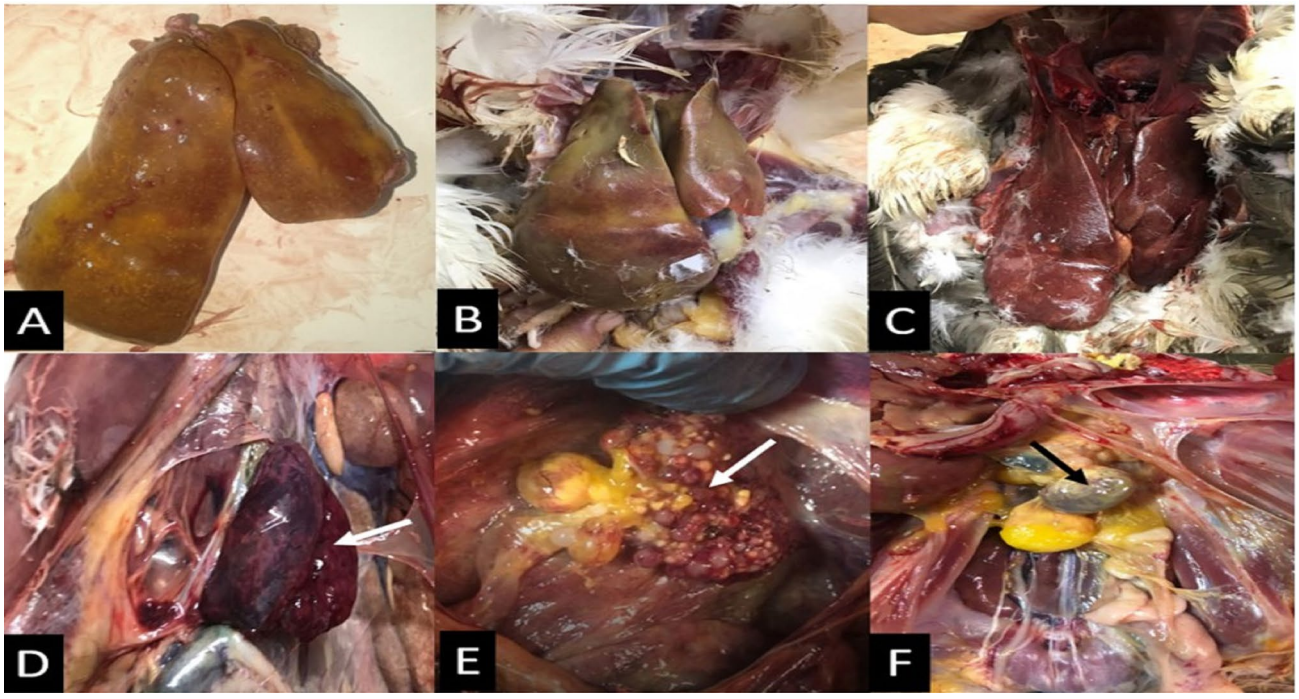

Fig. 2. Postmortem of freshly dead ducks shows: A& B: Severely enlarged liver of duck with subcapsular hemorrhage and fatty degeneration; C: Diffuse enlargement with congestion in the liver; D: Severely enlarged spleen of duck with severe congestion, subcapsular hemorrhage and rupture in the splenic capsule; E: Changes in the ovaries with miss shaped small size congested ova (arrow); F: Enlarged misshaped ovarian follicles with persistent bursa of Fabricius of breeder duck.

was observed with severe enlargement with yellowish color infiltration in the spleen (Fig. 2). The ovaries of some breeder ducks showed enlarged misshaped ovarian follicles with persistent bursa of Fabricius.

Histopathological findings

In chickens, microscopy of the kidney revealed severe peritubular infiltration with myeloid cells having eosinophilic granular cytoplasm (Fig. 3a). Neoplastic cells were pleomorphic with large-sized eccentric hyperchromatic oval nuclei. Mitotic figures were observed in cells. The tubular epithelium showed necrobiotic changes (Fig. 3b). Microscopy of the liver revealed multiple large irregular foci of myeloid cell infiltration displacing the hepatic cords. The hepatocytes suffered from necrobiotic changes (Figure 3c, d). Histopathological examination of the intestine showed myeloid cell infiltration in the lamina propria and submucosa (Fig. 3e). The lining epithelium of the intestinal villi was completely sloughed. Foci of myeloid cell infiltration were also observed in the tunica musculosa of the intestine (Fig. 7f). Microscopy of the pancreas revealed severe diffuse myeloid cell infiltration replacing the pancreatic acini associated with connective tissue proliferation (Fig. 3g). Microscopy of the ovary, on the other, revealed mild myeloid cell infiltration and showed oogenesis (Fig. 3h).

In ducks, microscopy of the liver revealed severe multifocal infiltration of myeloid cells with the replacement of hepatocytes and concentration around blood vessels (Figure 3i). The neoplastic cells had large eccentric nuclei with eosinophilic, mostly spherical granules in the cytoplasm. In the ovary, the myeloid cells infiltrated the interstitial tissue (Fig. 3j).

Real-time RT-PCR analysis

Liver, spleen, pancreas, and ovaries tissue samples were tested using qRT-PCR for the presence of ALV among different examined tissues, samples from duck tumors (liver, spleen) from Gharbia governorate (from a single farm) were positive. Samples from chickens (liver, spleen, and ovaries) from different farms within different governorates were positive. The Cq values were greatly different, indicating a different level of virus titers in the examined tissue. The lower Cq values were observed in the examined liver and spleen tissues, where samples from the pancreas and ovaries gave very late Cq values (Table 1).

The degree of infections in the different governorates based on qRT-PCR vary greatly; one out of five breeder duck samples (20%) from Gharbia governorates were positive for ALV, and the same results, 1 out of 5 (20%) were observed in the examined breeder chickens. In Damietta, 3/7-layer chicken farms (42.8%)

Table 4. The indel, GAPs and SNPs in the different positions in the five sequenced isolated of ALV

Position	Egy/YA- 2021.3	Egy/YA- 2021.4	Egy/YA- 2021.9	Egy/YA- 2021.10	Egy/YA- 2021.14	Mutation
1					C > A	- *
50				A > G		H > R
57				A > G		-
60					G > A	-
86				C > A		T > K
148			C > T	C > T		-
155				T > C		F > S
159			A > G			-
234			G > A	G > A		-
351				A > G		k > R
372			T > C	T > C		-
373	G > A	G > A				-
388	A > G	A > G				-
395		A > C				D >A
397				A > T		-
403		G < A				-
495				C > A		-
496	A > G	A > G				-
501	C > -					-
502	G > -					-
510				A > G		-
529	T > -					-
total SNPs per seq	3/0**	5 / 1	4/0	11/ 4	2/0	25/5
total GAPs per seq	3	0	0	0	0	

*The SNP has no effect on the amino acid level.

**The number of SNPs/ number of mutations that affects the amino acid

were positive for ALV. In Sharkia, 1/6 of breeder chicken farms (16.6%) were positive for ALV, and in Dakahlia, 1/4(25%) of breeder chicken farms were positive for ALV (Table 1).

Sequencing analysis of the envelope glycoprotein gene (gp85) of ALV virus

Five samples that tested positive for ALV using qRT-PCR were selected and subjected to sequencing of the *gp85* gene using Sanger sequencing technology; amplification of the *gp85* revealed a single band migrating at ~ 585 bp amplicon was seen in the teste samples. These amplicons were purified and subjected to sequencing.

Both nucleotide sequences and deduced amino acid sequence of the *gp85* gene of the 5 isolated Egyptian strains were aligned and analyzed (Figs. 4, 5 and 6); it was found that a total of 25 mutations spanning the five sequenced isolates have been detected with 20% (5 out of 25) affecting the level of amino acid, 44% of these nucleotide mutations found in one isolate (Egy/YA-2021.10) and had 80% effect on the level of the amino acid of this isolate. On the other hand, Isolate Egy/YA- 2021.4 had 20% of the total SNPs (5 out of 25) on the nucleotide level, with 20% influencing the amino acid level (Table 4).

Sequence analysis of the *gp85* revealed that nucleic acid identity ranges from 100% (strain 3 and 4) to a minimum of 97 % (strain 3 and 10, and strain 4 and 10); on the other hand, similarity (on deduced amino acid level) was varying greatly, between 99% (strain 9 and 14) to a minimum of 89% (strain 3 and 10) (Figs. 7 and 8)

The phylogenetic tree construction revealed that the strains of the current study belonged to one branch and were phylogenetically related to the strains isolated from Egypt in late 1999 and distinctly apparat from all chin stains. However, close to the strains of the UK and USA.

Construction of the phylogenetic tree based on the sequenced *gp85* gene retrieved from the Genbank (Table 5) revealed that all Egyptian isolates were neatly arranged in a single branch despite the year of collection and were phylogenetically distant from other sequences. Meanwhile, the duck sequence of the strain Egy/YA- 2021.9 was also grouped with the chicken isolates. In contrast, the duck sequence of China isolates was phylogenetically distant and grouped in a separate branch.

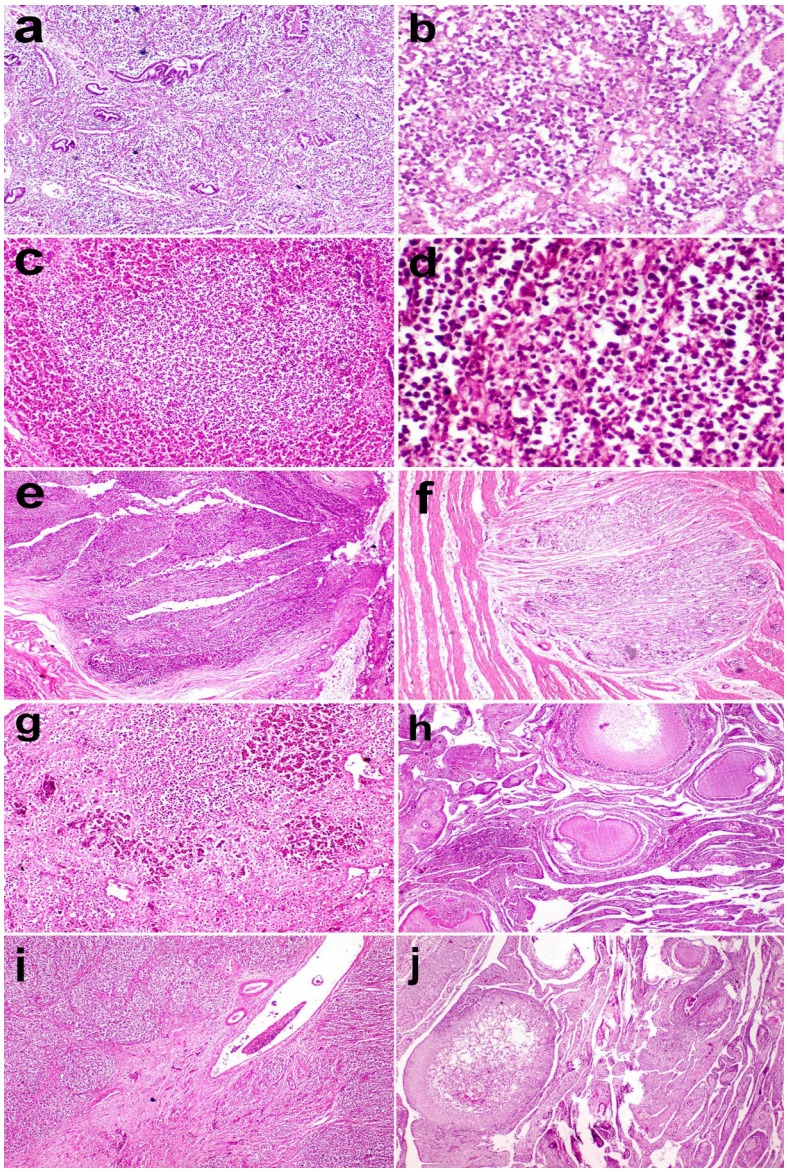

Fig. 3. The histopathological analysis of infected chicken with Avian Leukosis virus, (a) peritubular myeloid cells infiltration in the kidney (X100), (b) necrobiotic changes in the tubular epithelium (X200), (c) the focus of myeloid cells infiltration in the liver (X100), (d) cells had oval hyperchromatic eccentric nuclei and eosinophilic granular cytoplasm (X400), (e) myeloid cells infiltration in mucosa and submucosa of the intestine , (f) the focus of myeloid cells infiltration in the tunica musculosa of the intestine (X40), (g) diffuse myeloid cells infiltration and connective tissue proliferation in the pancreas replacing the glandular acini (X100), (h) mild myeloid cells infiltration in the ovary (40X). (i-j) The histopathology of organs in infected ducks with Avian Leukosis virus, (i) perivascular fibrosis and myeloid cells infiltration in the liver (X100), (j) myeloid cells infiltration in the interstitial tissue of the ovary (X100). Hematoxylin and eosin stain.

Analysis of the recombination events

The recombination events in the *gp85* gene of the five isolated Egyptian strains in the current study were analyzed by RDP5, and a single potential recombination event was detected (Fig. 9) in two isolates Egy/YA- 2021.3, and Egy/ YA-2021.4with the minor parent is isolate Egy/YA- 2021.14, This recombination event was supported by Bootscan, GENECONV, SiScan, and 3Seq methods. This event was found in the region of the *gp85* gene with a beginning breakpoint of 532 and an end breakpoint at 373 with 99% CI. The predicted minor parent Egy/YA.14 with global KA p-value 2.061= E-0.03 ($p<0.05$).

DISCUSSION

Avian leukosis virus is a serious vertically transmitted oncogenic virus that contaminates poultry vaccines and induces severe economic losses in the poultry sector in Egypt (Mousa and Abdel-Wahab 2009; Yehia *et al*., 2020; Gul *et al*., 2022). The observed clinical signs in this study did not differ greatly from other previous investigations that recorded by Kilany *et al*. (2015) and Eid *et al*. (2019); also, PM findings did not differ greatly as it revealed the presence of tumor lesions in different visceral organs with diffuse enlargement in the visceral organs including the liver, spleen, kidney, ovaries, bursa of Fabricius, and heart. Surprisingly, however, we find in the current study that the ovaries of the examined birds showed severe enlargement with deformity in ova shapes (miss-shaped ova) in contrast to the ovarian hypotrophy or even atrophy reported previously in previous Egyptian reports (Kilany *et al*., 2015). Also, the histopathological changes that were observed in the examined tissues were parallel to those recorded by Xu *et al*. (2004), El-Sebelgy *et al*. (2014), and Wen *et al*. (2018).

Most of the published molecular epidemiological studies focused on poultry. They reported that ducks, especially layer or broiler ducks, are rarely infected with ALV, however recently, many investigations, especially from China, focused on ALV infection in ducks (Li *et al*., 2013; Zeng *et al*., 2014a,b; Hao *et al*., 2014) and detected ALV subgroup A, B, E and J in migrating ducks and isolated Seven ALV-J strains from Northern Shoveller, Eurasian Wigeon, Baikal Teal and Green-winged Teal. In the current study, we could detect ALV-J in commercial breeder ducks in the Gharbia governorate with similar clinical findings and PM lesions as in

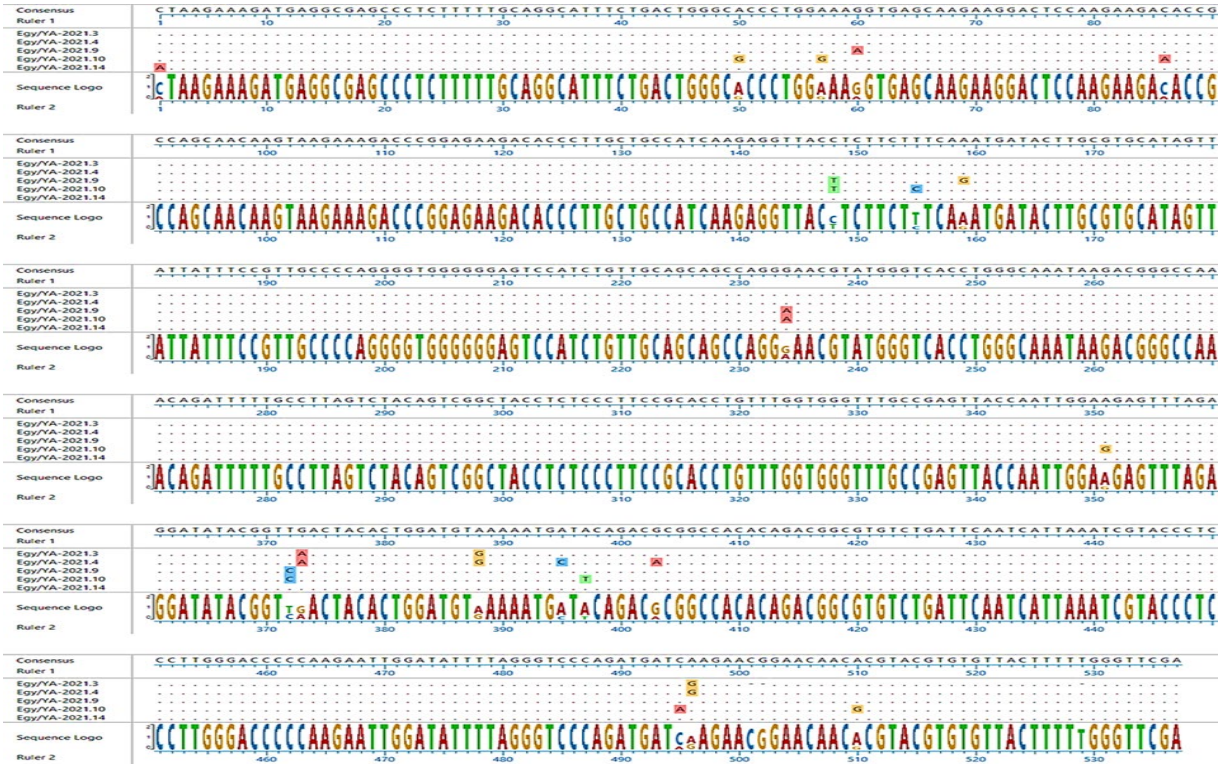

Fig. 4. The nucleotides sequence alignments of the sequenced *gp85* genes of the 5 ALV strains.

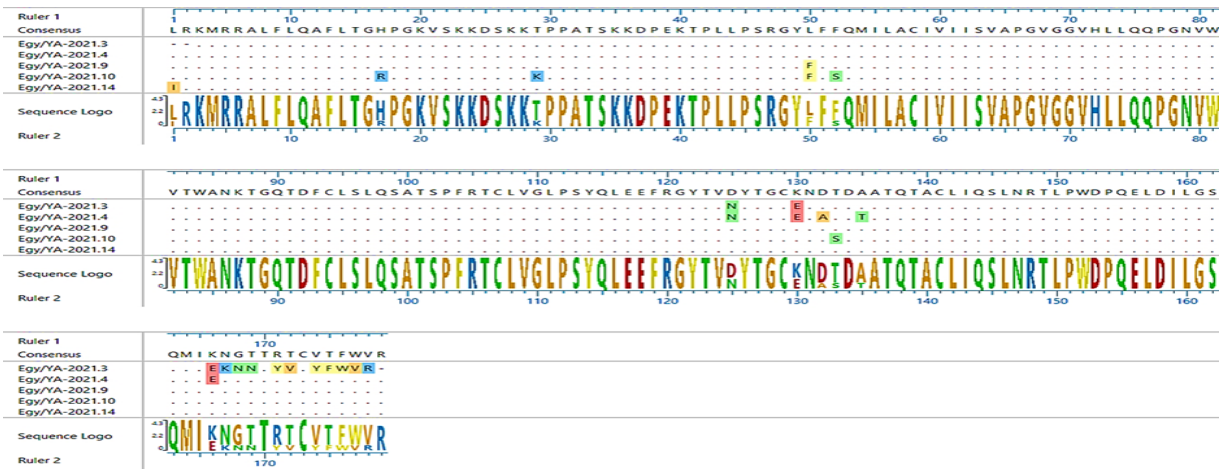

Fig. 5. The amino acid sequence alignments of the sequenced *gp85* genes of the 5 ALV strains.

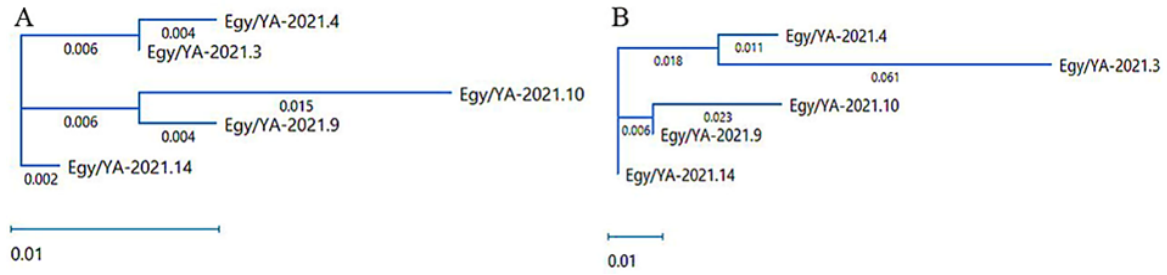

Fig. 6. The nucleotide (A) and deduced amino acid (B) phylogenetic tree contracted based on the sequence alignment of *gp85* of the 5 isolates of ALV.

Table 5. The strain name and accession number of the records used to construct the phylogenetic tree with the isolated strains of the current study.

Strain ID	Accession number	Host	Subgroup	Year of isolation	Country
Egy/YA- 2021.3	MZ614719	Chicken, indigenous layers	J	2021	Egypt
Egy/YA- 2021.9	MZ614720	Duck (subgroup J)	J	2021	Egypt
Egy/YA-2021.10	MZ614721	Chicken, indigenous breeders	J	2021	Egypt
Egy/YA-2021.14	MZ614722	Chicken, breeders	J	2021	Egypt
Egy/YA- 2021.4	MZ614723	Chicken, breeders	J	2021	Egypt
QL1 eg	MN496121	chicken	J	2019	Egypt
QL2 eg	MN496122	chicken	J	2019	Egypt
QL3 eg	MN496123	chicken	J	2019	Egypt
QL4 eg	MN496124	chicken	J	2019	Egypt
QL5 eg	MN496125	chicken	J	2019	Egypt
QL6 eg	MN496126	chicken	J	2019	Egypt
NG VX32	MH669346	Chicken contaminated vaccines	J	2018	Nigeria
NGVX29	MH669345	Chicken contaminated vaccines	J	2017	Nigeria
GD1403j	JX254901	Chicken blood plasma	J	2014	China
GD1402j	JX317565	Chicken blood plasma	J	2014	China
JS13LHAJ2	KR049127	Chicken, layer breeders	J	2013	China
WLY13	KJ631311	Chicken, broiler breeders	J	2013	China
WGZ13	KJ631313	Chicken, broiler breeders	J	2013	China
WGD13	KJ631312	Chicken, broiler breeders	J	2013	China
FJ201308	KM655822	Chicken, layers	J	2013	China
FJ201307	KM655821	Chicken, layers	J	2013	China
FJ201306	KM655820	Chicken, layers	J	2013	China
WSC112	KJ831322	Chicken, broiler breeders	J	2012	China
WL12	KJ631318	Chicken, broiler breeders	J	2012	China
WJ612	KJ631317	Chicken, broiler breeders	J	2012	China
WC512	KJ631316	Chicken, broiler breeders	J	2012	China
WA1112	KJ631315	Chicken, broiler breeders	J	2012	China
WB12062e	KJ009323	Duck	E	2012	China
WB11008e	JX570786	Baikal Teal (Duck)	E	2012	China
WB11098e	JX570792	Green winged Teal (Duck)	E	2012	China
WB11110e	JX570797	Baikal Teal (Duck)	E	2012	China
GD1109	JX254901	Chicken		2011	China
NHH	HM235668	Chicken, Layers		2010	China
JS-nt 1	HM235667	Chicken		2010	China
CAUHN01	HM640944	chicken		2009	China
ADOL 7501	AY027920	Chicken		2001	USA
TgM eg	DQ316906	meat type chicken		1999	Egypt
TgM 00	DQ316907	meat type chicken		1999	Egypt
TW99	AF497905	Chicken		1999	China
HPRS103	Z46390	Chicken		1994	U.K.

* The sequence was obtained from virus-infected secondary chicken embryo fibroblasts (CEF), The duck isolates highlighted in gray

the chicken.

Molecular testing of the collected chicken and duck samples for ALV-J using qRT-PCR revealed that different rates of ALV infections were detected, with a maximum infection rate of 42.8% in Damietta and a minimum of 16.6% in Sharkia governorates. The virus was detected in nearly all tested organs but with different concentrations (based on the Cq values). Coinfection with other oncogenic viruses like Reticuloendotheliosis virus and Marek's Disease viruses was omitted by testing the samples with real-time PCR using specific primers towards these viruses (Hassanin *et al*., 2013). This relatively high detection rate may be attributed to the usage of contaminated poultry vaccines, as recommended by Mohamed *et al*. (2010). Also, ALV was detected in another avian species in Egypt, as Bayoumi *et al*. (2021) reported.

A

		A	B	C	D	E
A	Egy/YA-2021.3		0.00	0.02	0.03	0.01
B	Egy/YA-2021.4	0.00		0.02	0.03	0.01
C	Egy/YA-2021.9	0.02	0.02		0.02	0.01
D	Egy/YA-2021.10	0.03	0.03	0.02		0.02
E	Egy/YA-2021.14	0.01	0.01	0.01	0.02	

B

	A	B	C	D	E
Egy/YA-2021.3		0.07	0.08	0.11	0.08
Egy/YA-2021.4	0.07		0.03	0.06	0.03
Egy/YA-2021.9	0.08	0.03		0.02	0.01
Egy/YA-2021.10	0.11	0.06	0.02		0.03
Egy/YA-2021.14	0.08	0.03	0.01	0.03	

Fig. 7. The nucleotide identity matrix (A) and deduced amino acid similarity matrix (B) based on the sequence alignment of the *gp85* of the 5 Egyptian isolates of ALV in the current study.

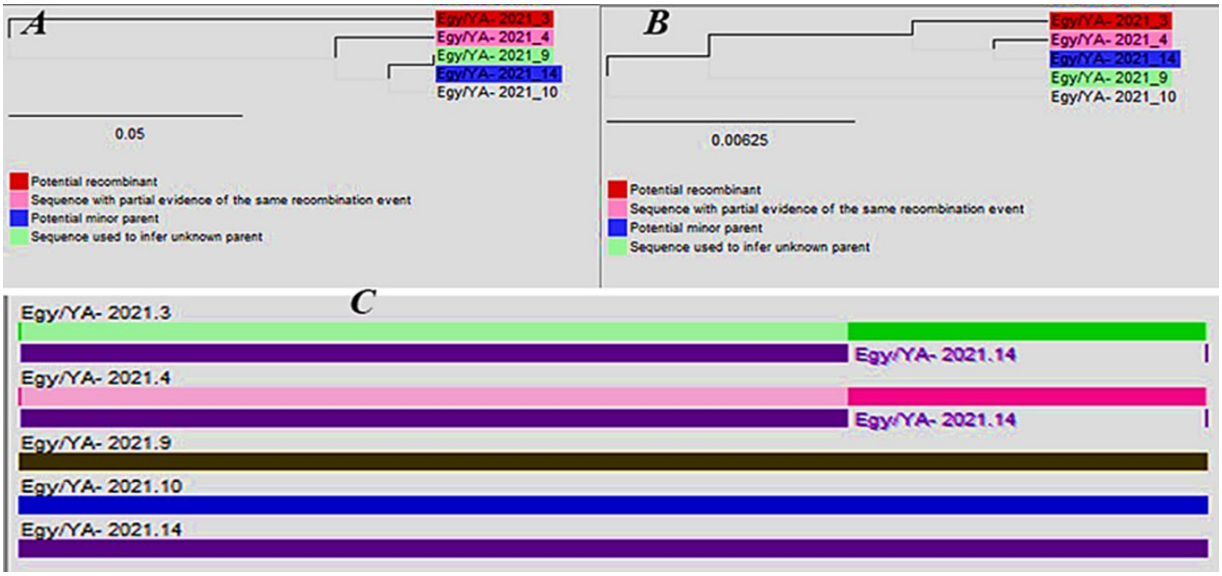

Fig. 8. UPGAMA of region derived from (A) the major parent (position 373- 532) and (B) minor parent (position 1-372 and 533- 54), (C) The position of the recombination events in the five ALV-J isolates.

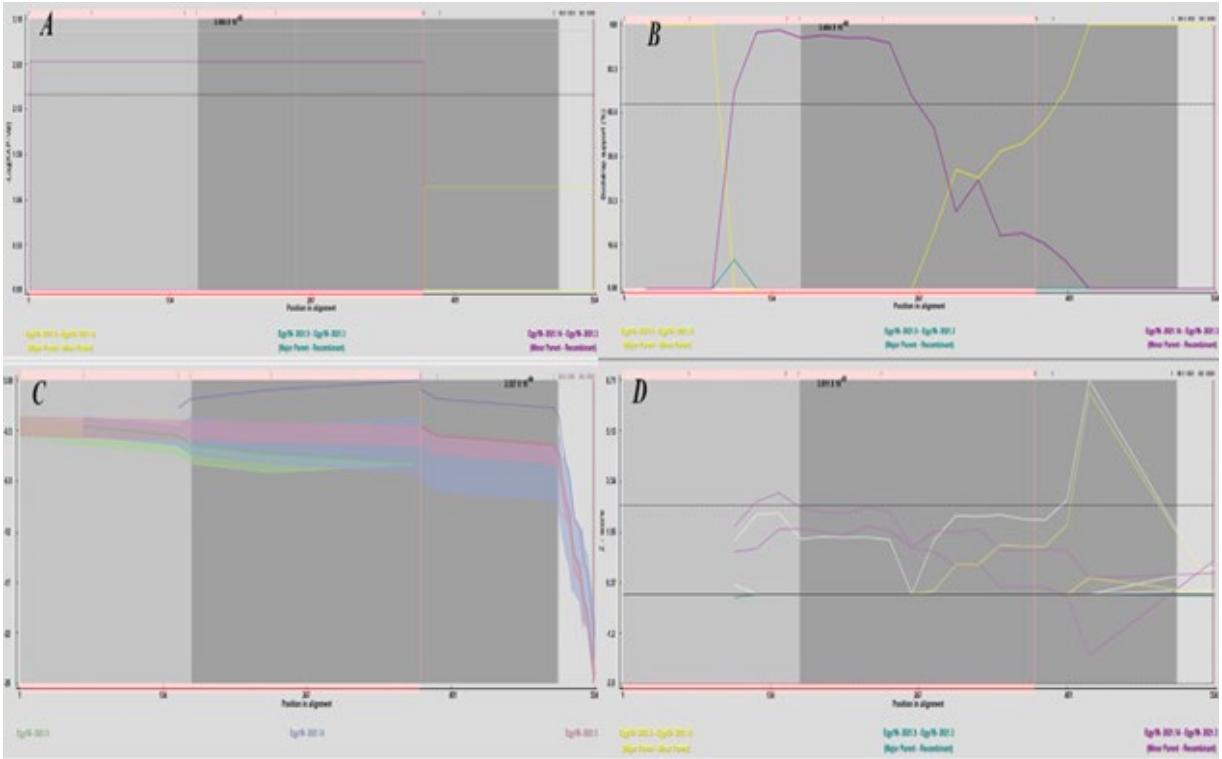

Fig. 9. Recombination event detection using GENECONV (A), BootScan (B), 3Seq (C) and SiScan (D) algorithms. The methods are based on pairwise distance model with a window size of 100, step size of 30, and 1,000 bootstrap replicates generated by the RDP5 program.

Subgroup specificity of the retrovirus is determined by the *gp85* sequence; mutation in such protein may result in changes in viral attachment affinity and viral entry with subsequent changes in viral transmission and both oncogenicity and pathogenicity, the analysis of amino acid mutations for the *gp85* genes of isolated strains in the current study reveal many amino acid substitutions (Přikryl *et al*., 2019). Out of 25 true SNPs detected among the 5 sequenced strains, only 5 SNPs had an impact on the amino acid and caused the mutation. The *env* genes of wild duck isolate from Gharbia governorate (Egy/YA- 2021.9) was significantly different from the sequences of other chicken isolate and from the prototype strain American strains HPRS-103.

Recombination event detection is very important in the follow-up of viral spread and pathogenesis.

Those recombination events- if present- lead to variation within ALV isolates that might trigger the widespread ALV infection (Fadly, 2000). In the current investigation, the chicken isolates only showed potential recombination events between two isolates, only explaining the complex evolutionary processes that may exist among ALVs that may be suggested that recombination might be the cardinal cause of ALV evolution. Other investigators adopted by Su *et al*. (2018) detected nearly the same rate of recombination events in ALV subgroup K whiten, the *pol* gene that is responsible for viral replication.

CONCLUSION

The circulating virulent AlV strains in Egypt from Dec 2020 until March was diagnosed with real-time RT-PCR, and five isolates were detected in the tested samples. The phylogenetic tree based on the nucleotide sequence and deduced amino acid sequence of the *gp85* gene revealed the presence of many mutations on the amino acid level and that these five isolates had a degree of variation. Recombination event analysis could detect a single event between two chicken isolates. Because there are currently no vaccinations or treatments for ALV and such a virus threatens poultry production, it is advised to eradicate the positive birds and do periodic molecular monitoring for the circulating Egyptian strains. Also, the whole genome sequence and analysis of these isolates are recommended to determine the pathogenicity and antigenicity of the recently isolated ALV-J strains.

CONFLICT OF INTEREST

The authors declare that they have no conflict of interest.

REFERENCES

Aydin, H., Smrke, B.M., Lee, J.E., 2013. Structural characterization of a fusion glycoprotein from a retrovirus that undergoes a hybrid 2-step entry mechanism. The FASEB Journal 27, 5059-5071.

Bancroft, J.D., Gamble, M., 2008. Theory and Practice of Histological Techniques. China: Elsevier health sciences.

Bande, F., Arshad, S.S., Omar, A.R. 2016. Isolation and metagenomic identification of avian leukosis virus associated with mortality in broiler chicken. Adv Virol. 15, 2016.

Bayoumi, M., El-Saied, M., Ahmed, B., El-Mahdy, M., Amer, H., 2021. Gallid alphaherpesvirus 2 in the Egyptian turkeys: molecular characterization and establishment of a universal system for phylogenetic classification. Intervirology 64, 156-64.

Cheng, J., Xu, Y., Zhou, D., Liu, K., Geng, N., Lu, J., Liu, Y., Liu, J., 2019. Novel carbon quantum dots can serve as an excellent adjuvant for the *gp85* protein vaccine against avian leukosis virus subgroup J in chickens. Poult. Sci. 98, 5315-20.

Delos, S.E., Godby, J.A., White J.M., 2005.Receptor-induced conformational changes in the SU subunit of the avian sarcoma/leukosis virus A *env*elope protein: implications for fusion activation. J. Virol., 79, 3488-3499.

Deng, Q., Li, M., He, C., Lu, Q., Gao, Y., Li, Q., Shi, M., Wang, P., Wei, P., 2021. Genetic diversity of avian leukosis virus subgroup J (ALV-J): toward a unified phylogenetic classification and nomenclature system. Virus Evol. 7, veab037.

Eid, A.E., Abd-Ellatieff, H.A., Ellakany, H.F., Abou-Rawash, A.R., AbdEl-Hamid, H.S., 2019. Studies on tumor disease viruses in chickens in Egypt. Alexandria Journal of Veterinary Sciences 60, 184-195.

El-Sebelgy, M.M., Ahmed, B.M., Ata, N.S., Hussein, H.A., 2014.Molecular detection and characterization of reticuloendotheliosis virus in broiler breeder chickens with visceral tumors in Egypt. Int. J. Vet. Sci. 2, 21-26.

Fadly, A.M., 2000. Isolation and identification of avian leukosis viruses: a review. Avian Pathol. 29, 529-535.

Gul, Zaib., Xuming, Hu., Hengmi, Cui., 2022. Global Maps of Avian Leukosis Viruses: Research Trends and Themes Based on Networking. Vet. Sci. 10, 16.

Guo, H.J., Li, H.M., Cheng, Z.Q., Liu, J.Z., Cui, Z.Z., 2010. Influence of REV and ALV-J co-infection on immunologic function of T lymphocytes and histopathology in broiler chickens. AGR. SCI. CHINA 9, 1667-1676.

Hao, R., Han, C., Liu, L., Zeng, X., 2014. First finding of subgroup-E avian leukosis virus from wild ducks in China. Vet. Microbiol. 173, 366-370.

Hassanin, O., Abdallah, F., El-Araby, I. E., 2013. Molecular characterization and phylogenetic analysis of Marek's disease virus from clinical cases of Marek's disease in Egypt. Avian Dis. 57, 555-561.

Jiang, L., Zeng, X., Hua, Y., Gao, Q., Fan, Z., Chai, H., Wang, Q., Qi, X., Wang, Y., Gao, H., Gao, Y., 2014. Genetic diversity and phylogenetic analysis of glycoprotein *gp85* of avian leukosis virus subgroup J wild-bird isolates from Northeast China. Arch. Virol. 159, 1821-1826.

Kilany, W.H., Soliman, M.A., Safwat, M., Mehana, O., El-Magid, M.A., Marwa, A.E., Hassan, M.K., Nasif, S.A., 2015. Detection of avian leukosis virus subgroup J from commercial Peking duck breeder farm in Egypt. Int. J. Virol. 11,139-145.

Li, D., Qin, L., Gao, H., Yang, B., Liu, W., Qi, X., Wang, Y., Zeng, X., Liu, S., Wang, X., Gao, Y., 2013. Avian leukosis virus subgroup A and B infection in wild birds of Northeast China. Vet. Microbiol. 163, 257-63.

Li, H., Cheng, Z., Liu, J., Liu, F., Guo, H., Cui, Z., 2009. Effect of co-infection with REV and ALV-J on T lymphocytes bioactivities and histopathology in broiler chickens. Sci. Agric. Sin. 42, 3296-304.

Li, T., Yao, X., Li, C., Zhang, J., Xie, Q., Wang, W., Lu, H., Fu, H., Li, L., Xie, J., Shao, H., 2020. Gp37 regulates the pathogenesis of avian leukosis virus subgroup J via its C terminus. J. Virol. 94, e02180-19.

Martin, D.P., 2009. Recombination detection and analysis using RDP3. In: Bioinformatics for DNA Sequence Analysis, 2009, Humana Press, pp. 185-205.

Martin, D.P., Posada, D., Crandall, K.A., Williamson, C., 2005a. A modified bootscan algorithm for automated identification of recombinant sequences and recombination breakpoints. AIDS Res. Hum. Retroviruses 21, 98-102.

Martin, D.P., Williamson, C., Posada, D., 2005b. RDP2: recombination detection and analysis from sequence alignments. Bioinformatics 21, 260-262.

McNally, M.M., Wahlin, K.J., Canto-Soler, M.V., 2010. Endogenous expression of ASLV viral proteins in specific pathogen free chicken embryos: relevance for the developmental biology research field. BMC Dev. Biol. 10, 1-1.

Meng, F., Dong, X., Hu, T., Chang, S., Fan, J., Zhao, P., Cui, Z., 2016. A deep sequencing reveals significant diversity among dominant variants and evolutionary dynamics of avian leukosis viruses in two infectious ecosystems. BMC Vet. Res. 12, 1-0.

Meng, F., Li, Q., Han, R., Xu, G., Gao, X., Luo, F., Shen, G., Liu, X., Zhang, Z., Zhao, P., Zhang, G. 2022. A study on the infection status and transmission of avian leukosis virus subgroup J in Hy-line brown roosters. Arch. Virol. 23, 1-7.

Mohamed, M.A., Abd El-Motelib, T.Y., Ibrahim, A.A., El-Deen, M.E., 2010. Contamination rate of avian leukosis viruses among commercial Marek's disease vaccines in Assiut, Egypt market using reverse transcriptase-polymerase chain reaction. Vet. World 3, 8.

Mousa, S., Abdel-Wahab, M.H., 2009. Prevalence of avian leukosis virus in chicken flocks in upper Egypt. Assiut Vet. Med. J. 55, 1-9.

Ottiger, H.P., 2010. Development, standardization and assessment of PCR systems for purity testing of avian viral vaccines. Biologicals. 38, 381-388.

Pan, W., Gao, Y., Qin, L., Ni, W., Liu, Z., Yun, B., Wang, Y., Qi, X., Gao, H., Wang, X., 2012. Genetic diversity and phylogenetic analysis of glycoprotein *Gp85* of ALV-J isolates from Mainland China between 1999 and 2010: coexistence of two extremely different subgroups in layers. Vet. Microbiol. 156, 205-212.

Přikryl, D., Plachý, J., Kučerová, D., Koslová, A., Reinišová, M., Šenigl, F., Hejnar, J. 2019. The novel avian leukosis virus subgroup K shares its cellular receptor with subgroup A. J. Virol. 93, e00580-19.

Qiao, D., He, Q., Cheng, X., Yao, Y., Nair, V., Shao, H., Qin, A., Qian, K., 2021. Regulation of Avian Leukosis virus subgroup J replication

by Wnt/β-catenin signaling pathway. Viruses 13, 1968.

Qin, L., Gao, Y., Ni, W., Sun, M., Wang, Y., Yin, C., Qi, X., Gao, H., Wang, X., 2013. Development and application of real-time PCR for detection of subgroup J avian leukosis virus. J. Clin. Microbiol. 51,149-54.

Qu, Y., Liu, L., Niu, Y., Qu, Y., Li, N., Sun, W., Lv, C., Wang, P., Zhang, G., Liu, S., 2016. Viral proliferation and expression of tumor-related gene in different chicken embryo fibroblasts infected with different tumorigenic phenotypes of avian leukosis virus subgroup J. Poult. Sci. 95, 2383-2390.

Sacco, M.A., Howes, K., Smith, L.P., Nair, V.K., 2004. Assessing the roles of endogenous retrovirus EAV-HP in avian leukosis virus subgroup J emergence and tolerance. J. Virol. 78, 10525-10535.

Shen, Y., Cai, L., Wang, Y., Wei, R., He, M., Wang, S., Wang, G., Cheng, Z., 2014. Genetic mutations of avian leukosis virus subgroup J strains extended their host range. J. Gen. Virol. 95, 691-699.

Su, Q., Li, Y., Li, W., Cui, S., Tian, S., Cui, Z., Zhao, P., Chang, S., 2018. Molecular characteristics of avian leukosis viruses isolated from indigenous chicken breeds in China. Poult. Sci. 97, 2917-2925.

Tang, S., Li, J., Chang, Y.F., Lin, W., 2022. Avian Leucosis Virus-Host Interaction: The Involvement of Host Factors in Viral Replication. Front. immunol. 13, 907287

Wang, P., Lin, L., Li, H., Yang, Y., Huang, T., Wei, P., 2018. Diversity and evolution analysis of glycoprotein *Gp85* from avian leukosis virus subgroup J isolates from chickens of different genetic backgrounds during 1989-2016: coexistence of five extremely different clusters. Arch. Virol. 163, 377-89.

Wen, Y., Huang, Q., Yang, C., Pan, L., Wang, G., Qi, K., Liu, H., 2018. Characterizing the histopathology of natural co-infection with Marek's disease virus and subgroup J avian leucosis virus in egg-laying hens. Avian Pathol. 47, 83-89.

Wu, L., Li Y, Chen, X., Yang, Y., Fang, C., Gu, Y., Liu, J., Liang, X., Yang, Y., 2022. Isolation and characterization of avian leukosis virus subgroup J associated with hemangioma and myelocytoma in layer chickens in China. Front. Vet. Sci. 9.

Xu, B., Dong, W., Yu, C., He, Z., Lv, Y., Sun, Y., Feng, X., Li, N. F., Lee, L., Li, M., 2004. Occurrence of avian leukosis virus subgroup J in commercial layer flocks in China. Avian Pathol. 33, 13-17.

Yehia, N., El-Sayed, H.S., Omar, S.E., Amer, F., 2020. Genetic variability of the Avian leukosis virus subgroup J *gp85* gene in layer flocks in Lower Egypt. Vet. World 13, 1065.

Zeng, X., Gao, Y., Li, D., Hao, R., Liu, W., Han, C., Gao, H., Qi, X., Wang, Y., Liu, L., Wang, X., 2014a. Molecular characteristics of the complete genome of a J-subgroup avian leukosis virus strain isolated from Eurasian teal in China. Virus genes 49, 250-258.

Zeng, X., Liu, L., Hao, R., Han, C., 2014b. Detection and molecular characterization of J subgroup avian leukosis virus in wild ducks in China. PloS One 9, e94980.